

# Hierarchical Black Hole Mergers in Nuclear Star Clusters: A Combined Dynamical-Secular Channel for GW231123-like Events

Bin Liu<sup>1,2,\*</sup> and Dong Lai<sup>3,4</sup>

<sup>1</sup>*Institute for Astronomy, School of Physics, Zhejiang University, Hangzhou 310027, China*

<sup>2</sup>*Center for Cosmology and Computational Astrophysics,*

*Institute for Advanced Study in Physics, Zhejiang University, Hangzhou 310027, China*

<sup>3</sup>*Tsung-Dao Lee Institute, Shanghai Jiao Tong University, Shanghai 200240, China*

<sup>4</sup>*Department of Astronomy, Center for Astrophysics and Planetary Science, Cornell University, Ithaca, NY 14853, USA*

The recent binary black hole (BH) merger GW231123, with both components likely in the high-mass gap and with high spins, challenges standard BH binary formation models. It is usually thought that the BHs are of second (or higher) generation (2G), resulting from the mergers of smaller BHs. But the physical processes that produce the merging 2G BH binaries are unclear and highly unconstrained. We show that such 2G mergers can be naturally produced in the nuclear star cluster of Milky Way-like galaxy. The dominant channel combines a sequence of binary-single interactions with secular evolution driven by the central supermassive BH. Our model produces a merger rate consistent with GW231123 and further predicts an abundant population of 2G BH-star (or low-mass BH) binaries; these binaries may observationally manifest as micro tidal disruption events or low-frequency gravitational-wave (GW) sources. Detecting these binaries would provide crucial insights into the dynamical pathways of hierarchical BH assembly.

*Introduction.*— The fourth observing run of the LIGO-Virgo-KAGRA Collaboration has significantly expanded the GW transient catalog, bringing the total number of detected compact binary mergers to over 200 [1]. While events like GW190521 provided initial evidence for hierarchical BH mergers [2], the recent detection of GW231123 presents a more profound challenge to standard binary evolution models [3–12]. This BH binary (BHB) merger features components with masses  $m_1 = 137_{-17}^{+22} M_\odot$  and  $m_2 = 103_{-52}^{+20} M_\odot$  and spin parameters  $\chi_1 = 0.9$  and  $\chi_2 = 0.8$ , indicating that both likely lie in the so-called “high-mass gap”. The combination of high masses and high spins is inconsistent with first-generation (1G) BHs born from direct stellar collapse, suggesting that GW231123 is a merger between two second-generation (2G) or higher generation BHs, each likely the remnant of a previous BH merger [13–22].

Nuclear star clusters (NSCs) and active galactic nuclei (AGN) disk, with their deep potential wells and high stellar densities, are promising locations for such hierarchical growth [23–46]. These dense environments foster frequent dynamical encounters, and the high escape velocities aid in retaining 2G BHs. However, how to form bound and merging 2G/2G BHBs is not straightforward. In particular, in NSC, a newly formed 2G/2G binary is typically too wide (“soft”) to merge before being disrupted by subsequent scattering interactions [47–58].

In this *letter*, we propose a novel channel in NSC that resolves this tension by combining dynamical interaction with secular evolution. Using semi-analytical models, we demonstrate that the formation of merging 2G/2G binaries requires a two-step process: first, rapid dynamical interactions such as binary-single exchanges form wide but bound 2G/2G binaries; second, the von Zeipel-Lidov-Kozai effect induced by the central supermassive

BH (SMBH) drives these binaries to high eccentricities [59–75], enabling rapid merger and avoiding disruption.

*Dynamical process.*— The evolution of BH systems in dense environments like NSCs involves complex dynamics, governed by the SMBH’s tidal gravity, multi-body scatterings and secular interactions [76]. To clarify the formation pathways of 2G/2G BHB mergers, we focus on three representative dynamical channels, illustrated in Fig. 1, while leaving more complex interactions such as binary–binary scattering for future studies.

We model the NSC with three distinct populations. The stellar component with mass  $m_s (\simeq 1M_\odot)$  follows a power-law density cusp [77],

$$n_s \equiv n_0 \left( \frac{R}{\text{pc}} \right)^{-\gamma} = \frac{1.35 \times 10^6 M_\odot}{\text{pc}^3} \left( \frac{R}{0.25 \text{ pc}} \right)^{-\gamma}, \quad (1)$$

where  $n_0$  is the normalized density at distance  $R = 0.25 \text{ pc}$  and  $\gamma$  is the slope of the density distribution. This profile agrees with recent observational constraints for the Galactic center [78]. The differential number of stars within a shell at  $R$  follows as  $dN_s = 4\pi n_0 R^{3-\gamma} d \ln R$ . The one-dimensional velocity dispersion,  $\sigma_s = \sqrt{GM_\bullet/[R(1+\gamma)]}$ , is set by the SMBH of mass  $M_\bullet$  [79, 80], and the SMBH’s influence radius  $R_{\text{inf}} = GM_\bullet/\sigma_s^2$ . Stellar binaries are included with a number density  $n_b = f_b n_s$  (with fiducial value  $f_b = 10\%$ ) and each binary has mass  $\simeq 2M_\odot$ . We assume there exists a steady population of 2G BHs in the cluster, with number density  $n_{2G} = f_{2G} n_s$  (fiducial value  $f_{2G} = 0.05\%$ ) and individual mass  $m_{2G} \simeq 100M_\odot$ . After mass segregation, all populations share similar velocity dispersions,  $v_s \simeq v_b \simeq v_{2G} \simeq \sigma_s$  at radius  $R$ . This three-population model is highly idealized (e.g., it neglects the difference in the density profiles of different populations [81–83]; it neglects the other populations of different masses), but

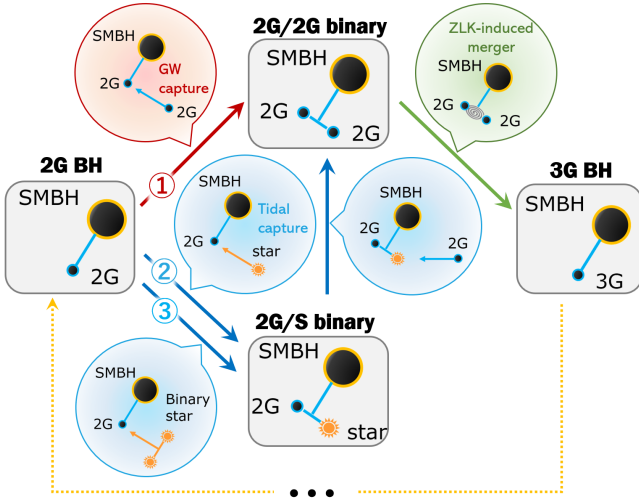


FIG. 1. Dynamical pathways for 2G/2G mergers in NSCs. The evolution begins with a 2G BH (left), which may form a 2G/2G binary through GW capture (Channel 1). Alternatively, it can first form a 2G/star (S) binary via tidal capture (Channel 2) or binary–single (S/S binary-2G) interaction (Channel 3), followed by an exchange interaction with another 2G BH that yields a 2G/2G binary. This binary then merges into a 3G BH driven by secular forcing from the SMBH (ZLK effect), potentially initiating further hierarchical growth.

it allows us to evaluate the relative importance of various key dynamical processes. In this work, the notation “ $A/B$ ” denotes a binary with component  $A$  and  $B$ , and “ $A-B$ ” indicates a dynamical encounter between  $A$  and  $B$ .

*Channel 1: Gravitational wave capture.* The first channel is the dynamical formation of a 2G/2G binary through GW emission. Consider two 2G BHs approach each other with velocity  $v_{2G} \simeq \sigma_s$  (at  $R \simeq \infty$ ) and the closest approach distance  $r_{\text{int}}$ . The radiated GW energy is  $\Delta E_{\text{GW}}(r_{\text{int}}) \simeq (85\pi/12\sqrt{2})[G^{7/2}\mu_{2G,2G}^2(2m_{2G})^{5/2}]/[c^5(r_{\text{int}}^{\text{GW}})^{7/2}]$ . To form a bound 2G/2G binary requires  $(1/2)\mu_{2G,2G}v_{2G}^2 - \Delta E_{\text{GW}}(r_{\text{int}}) = E_b \equiv -Gm_{2G}^2/(2a_{2G/2G}^{\text{GW}}) \lesssim 0$ . To avoid disruption of the 2G/2G binary by subsequent stellar encounters requires  $E_b \lesssim -m_s v_s^2/2$ . This implies that the 2G/2G binary has a characteristic semi-major axis

$$a_{2G/2G}^{\text{GW}} \simeq \frac{Gm_{2G}^2}{m_s v_s^2}. \quad (2)$$

The required interaction distance  $r_{\text{int}}^{\text{GW}}$  is set by  $\Delta E_{\text{GW}}(r_{\text{int}}) \simeq m_s v_s^2$ , giving  $r_{\text{int}}^{\text{GW}} = (85\pi/12)^{2/7}[m_{2G}c^2/(m_s v_s^2)]^{2/7}(Gm_{2G}/c^2)$ . The corresponding cross section for binary formation is  $\sigma_{2G-2G} \simeq \pi(v_{\text{int}} r_{\text{int}}^{\text{GW}}/v_s)^2$ , where  $v_{\text{int}} \simeq (4Gm_{2G}/r_{\text{int}}^{\text{GW}})^{1/2}$ . The timescale for 2G/2G binary formation is

$$T_{2G-2G} \simeq v_s(4\pi Gm_{2G}n_{2G}r_{\text{int}}^{\text{GW}})^{-1}. \quad (3)$$

The captured 2G/2G binary has an eccentricity given by

$a_{2G/2G}^{\text{GW}}(1 - e_{2G/2G}^{\text{GW}}) \simeq r_{\text{int}}^{\text{GW}}$ , and merges quickly [84].

*Channel 2: Tidal capture.* A 2G BH may form a binary with another 2G BH through a two-step process. It first tidally captures a star to form an intermediate 2G/star (2G/S) binary. The timescale for this 2G–S encounter is

$$T_{2G-S} \simeq v_s(2\pi Gm_{2G}n_s r_{\text{int}}^{\text{tide}})^{-1}, \quad (4)$$

where  $r_{\text{int}}^{\text{tide}}$  is the pericenter distance for significant tidal energy dissipation ( $\Delta E_{\text{tide}}$ ). We adopt  $\Delta E_{\text{tide}} \simeq (Gm_{2G}^2/R_s)(R_s/r_{\text{int}}^{\text{tide}})^6(A\eta^{-\beta})$  with  $A = 0.24$ ,  $\beta = 3.1$  appropriate for a polytrope of index 4/3,  $R_s$  the stellar radius and  $\eta \simeq (m_s/m_{2G})^{1/2}(r_{\text{int}}^{\text{tide}}/R_s)^{3/2}$  [85, 86]. Setting  $\Delta E_{\text{tide}} \simeq m_s v_s^2$ , we have  $r_{\text{int}}^{\text{tide}} \simeq [AGm_s/(v_s^2 R_s)]^x R_s (m_{2G}/m_s)^y$  with  $x = 2/(12+3\beta)$  and  $y = (4+\beta)/(12+3\beta)$ .

A bound, hard 2G/S binary forms if its binding energy satisfies  $|Gm_{2G}m_s/(2a_{2G/S}^{\text{tide}})| \gtrsim m_s v_s^2/2$ , yielding a characteristic semi-major axis

$$a_{2G/S}^{\text{tide}} \simeq \frac{Gm_{2G}}{v_s^2}. \quad (5)$$

Gravitational scatterings with other stars then harden the binary to  $a_{2G/S}^{\text{tide}} \simeq a_{2G/S}^{\text{tide}}/2$ . This 2G/S binary may further experience a binary–single exchange interaction when another 2G BH approaches within a distance  $\sim a_{2G/S}^{\text{tide}}$ . The encounter timescale is:

$$T_{2G/S-2G} \simeq v_s(4\pi Gm_{2G}n_{2G}a_{2G/S}^{\text{tide}})^{-1}. \quad (6)$$

During the interaction, an energy exchange of order  $\Delta E \simeq Gm_{2G}m_s/a_{2G/S}^{\text{tide}}$  occurs. If the lighter star is ejected with sufficiently large energy, a 2G/2G binary forms. The binding energy of the new binary satisfies  $Gm_{2G}^2/(2a_{2G/2G}^{\text{tide}}) \simeq \Delta E/2$ , giving the characteristic semi-major axis

$$a_{2G/2G}^{\text{tide}} \simeq \frac{Gm_{2G}^2}{m_s v_s^2}. \quad (7)$$

The corresponding eccentricity follows from  $a_{2G/2G}^{\text{tide}}(1 - e_{2G/2G}^{\text{tide}}) \simeq a_{2G/S}^{\text{tide}}$ . The resulting 2G/2G binary is relatively soft that could be disrupted by subsequent scatterings, with an evaporation timescale [87, 88]:

$$T_{\text{evap}} \simeq \left(\frac{m_{2G}}{m_s}\right)^2 \left[ n_s \pi \left( \frac{4Gm_{2G}a_{2G/2G}^{\text{tide}}}{v_s} + (a_{2G/2G}^{\text{tide}})^2 v_s \right) \right]^{-1}. \quad (8)$$

Only the binaries that can merge within  $T_{\text{evap}}$  are taken into account in our rate estimate (see below).

*Channel 3: Binary-single interaction.* A third channel for 2G/2G mergers involves binary–single (BS) interaction between a 2G BH and a stellar binary. Consider stellar binaries with semi-major axis  $a_{s/s} \simeq Gm_s/v_s^2$ . The binary–2G encounter timescale is

$$T_{2G-S/S} \simeq v_s(2\pi Gm_{2G}n_{\text{bs}}r_{\text{int}}^{\text{BS}})^{-1}, \quad (9)$$

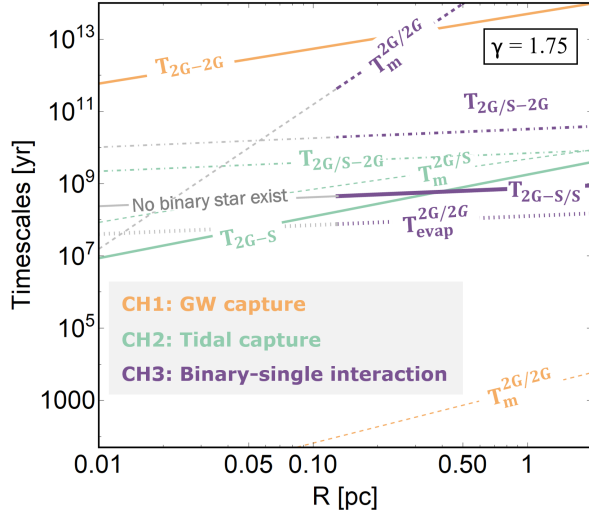


FIG. 2. Key timescales for forming 2G/2G mergers via different channels, evaluated at distance  $R$  from an SMBH of mass  $M_\bullet = 4 \times 10^6 M_\odot$ , assuming a density profile index  $\gamma$  constant for all populations. The merger time of various binaries due to GW emission (without the influence of the SMBH) are denoted by  $T_m$ .

with the interaction distance  $r_{\text{int}}^{\text{BS}} \simeq a_{s/s}(m_{2G}/m_s)^{1/3}$ .

This tidal disruption process, analogous to the Hill mechanism, releases energy  $\Delta E \simeq Gm_{2G}m_s a_{s/s}/(r_{\text{int}}^{\text{BS}})^2$ , typically producing a bound 2G/S binary and ejecting the other star. The 2G/S binary’s semi-major axis can be evaluated by  $Gm_{2G}m_s/(2a_{2G/S}^{\text{BS}}) \simeq \Delta E/2$  [89]:

$$a_{2G/S}^{\text{BS}} \simeq \frac{Gm_s}{v_s^2} \left( \frac{m_{2G}}{m_s} \right)^{2/3}. \quad (10)$$

Scattering with field stars hardens the binary to  $a_{2G/S}^{\prime\text{BS}} \simeq a_{2G/S}^{\text{BS}}/2$ . A subsequent encounter with another 2G BH, occurring over a timescale  $T_{2G/S-2G}$  (Eq. 6 with  $a_{2G/S}^{\prime\text{tide}} \rightarrow a_{2G/S}^{\prime\text{BS}}$ ), has a finite probability of forming a 2G/2G binary. The resulting binary has a characteristic semi-major axis:

$$a_{2G/2G}^{\text{BS}} \simeq \frac{Gm_{2G}}{v_s^2} \left( \frac{m_{2G}}{m_s} \right)^{2/3}. \quad (11)$$

As before, the binary may be disrupted by later encounters; only those that merge within  $T_{\text{evap}}$  (Eq. 8 with  $a_{2G/2G}^{\text{tide}} \rightarrow a_{2G/2G}^{\text{BS}}$ ) contribute to the detection rate.

Fig. 2 compares the timescales for 2G/2G binary formation through different channels. In the GW capture channel (orange), the 2G–2G encounter timescale is long, but once formed, the binary merges rapidly. For tidal capture (green), the ratio  $T_m^{2G/S}/T_{2G/S-2G} \ll 1$  indicates that 2G/S binaries merge before encountering another 2G BH. These mergers may potentially produce micro tidal disruption events, making this channel ineffective for 2G/2G binary production. The binary–single

channel operates mainly at larger galactic distance  $R$ , where stellar binaries survive ( $a_{s/s} \gtrsim 2R_s$ ). A newly formed 2G/S binary may undergo an exchange interaction to form a 2G/2G binary, but the resulting system can be easily disrupted by the subsequent scatterings ( $T_m/T_{\text{evap}} \gg 1$ ). However, including the ZLK effect from the SMBH can increase the eccentricity and accelerate mergers, with  $T_m^{\text{ZLK}} \simeq T_{m,0}(1 - e_{\text{max}}^2)^3$ , where  $T_{m,0} \equiv [5c^5 a_{2G/2G}^4]/[256G^3(2m_{2G/2G})^2 \mu_{2G,2G}]$  and  $e_{\text{max}}$  is the maximum eccentricity attained through ZLK oscillations [13, 69, 90, 91]. Our analysis includes both GW-driven orbital decay and ZLK-induced merger mechanisms across all channels. Note that for 2G/S binaries, the small semi-major axis strongly suppresses the ZLK effect, giving  $T_m \simeq T_m^{\text{ZLK}}$ . In contrast, for 2G/2G binaries, the ZLK effect becomes efficient due to large  $a_{2G/2G}^{\text{BS}}$  – This is often essential for achieving merger before evaporation.

*Merger rate.* – To quantitatively assess each channel’s contribution to 2G/2G mergers, we develop a multi-stage evolutionary model where 2G BHs evolve sequentially through pairing and merger phases. For the tidal capture and binary–single interaction channels, we track four “intermediate populations”: single 2G BHs ( $N_{2G}$ ), 2G/S binaries ( $N_{2G/S}$ ), 2G/2G binaries ( $N_{2G/2G}$ ), and third-generation (3G) BHs ( $N_{3G}$ ). For a typical galaxy, their evolution is governed by a set of equations:

$$\begin{cases} \frac{dN_{2G/S}}{dt} = \frac{N_{2G}}{T_A} - \frac{N_{2G/S}}{T_B} \\ \frac{dN_{2G/2G}}{dt} = f_1 \frac{N_{2G/S}}{T_B} - \frac{N_{2G/2G}}{T_m} \\ \frac{dN_{3G}}{dt} = f_2 \frac{N_{2G/2G}}{T_m}. \end{cases} \quad (12)$$

Here,  $T_A \equiv T_{2G-S}$  (tidal capture) or  $T_{2G-S/S}$  (binary single interaction),  $T_B \equiv T_{2G/S-2G}$ ;  $f_1$  and  $f_2$  denote the probability of forming a 2G/2G binary after a 2G/S–2G interaction and the fraction of systems merging via the ZLK mechanism, respectively. We use  $f_1 \simeq 10\%$  for our fiducial value, and calculate  $f_2$  using the method of [13]. We assume that there is a steady production of 2G BHs, so that  $N_{2G} = \text{const}$ . In steady state, the merger rate  $\Gamma = dN_{3G}/dt$  at a given distance  $R$  can be obtained analytically. See Appendix A for details, including the GW capture channel.

The top panel of Fig. 3 shows the merger rates for the GW capture and binary–single channels. Tidal capture is excluded since 2G/S binaries merge before encountering another 2G BH (Fig. 2). These rates depend sensitively on  $\gamma$ , which sets the stellar density  $n_s$  and encounter timescales. The GW capture channel is inefficient, due to the long 2G–2G encounter timescale  $T_{2G-2G}$ , with the rate  $10^2 \sim 10^3$  times lower than the binary–single channel. For the binary–single interaction, we exclude the distance ranges where stellar binaries cannot survive or where the 2G/S binary merges within  $T_{2G/S-2G}$ . For the remaining 2G/2G binaries, the ZLK mechanism plays an important role in accelerating the mergers, but only a

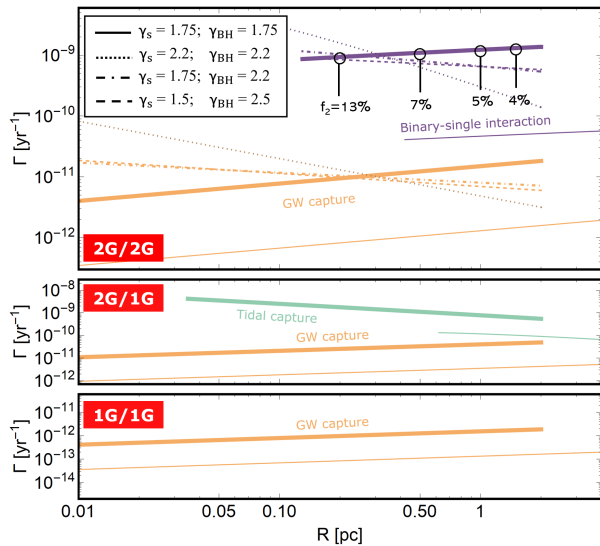


FIG. 3. Top panel: 2G/2G BHB merger rates versus the galactic distance  $R$ . The rates are derived per galaxy from Eq. (12). Different slopes of the density profile for star ( $\gamma_s$ ) and BH ( $\gamma_{\text{BH}}$ ) are taken into account (as labeled; see Eq. 1). We adopt  $f_1 = 10\%$  and  $T_m = T_{\text{evap}}$  in Eq. (12);  $f_2$  denotes the fraction of systems that reach eccentricities high enough to merge within  $T_{\text{evap}}$  (ZLK window), calculated assuming isotropic orbital orientations [13]. Middle/Bottom panels: 2G/1G and 1G/1G merger rates for  $\gamma = 1.75$ . Thick solid lines correspond to  $M_\bullet = 4 \times 10^6 M_\odot$  and thin solid lines represent  $M_\bullet = 10^7 M_\odot$ .

fraction  $f_2 \lesssim 15\%$  satisfy  $T_m^{\text{ZLK}} \lesssim T_{\text{evap}}$ . We find that, when scaled to the number of Milky Way-like galaxies in the local universe [92, 93], the binary–single encounters yields a merger rate consistent with the inferred rate of GW231123 (See Appendix A).

We now consider an additional population, 1G BHs in NSCs, with masses below the high-mass gap ( $\lesssim 60M_\odot$ ). We adopt a representative mass of  $10M_\odot$  and a density  $n_{1G} = f_{1G}n_s$  with fiducial  $f_{1G} = 1\%$ . For the GW capture channel, the 2G/1G merger rate is computed as in the 2G/2G case (See Appendix B), giving a characteristic semi-major axis for 2G/1G binaries:

$$a_{2G/1G}^{\text{GW}} \simeq \frac{Gm_{2G}m_{1G}}{m_s v_s^2}. \quad (13)$$

For the tidal capture and binary–single channels, we apply a similar analysis but replace the interaction with a second 2G BH by that with a 1G BH. A 2G/S binary may thus undergo an exchange interaction with a 1G BH, forming a 2G/1G binary. The characteristic semi-major axes are:

$$a_{2G/1G}^{\text{tide}} \simeq \frac{Gm_{1G}}{v_s^2} \frac{m_{2G}}{m_s}, \quad a_{2G/1G}^{\text{BS}} \simeq \frac{Gm_{1G}}{v_s^2} \left( \frac{m_{2G}}{m_s} \right)^{2/3}. \quad (14)$$

As with 2G/2G binaries, these 2G/1G systems are generally soft and vulnerable to disruption by stellar scatter-

ings, strongly limiting their merger efficiency. We compute the 1G/1G merger rates in the same way as the 2G/2G case, with 1G BHs replacing 2G BHs.

The middle and bottom panels of Fig. 3 show that for  $M_\bullet = 4 \times 10^6 M_\odot$ , the binary–single channel produces few 2G/1G mergers. The 2G/1G binaries have smaller semi-major axes than 2G/2G systems ( $a_{2G/1G}^{\text{BS}} \ll a_{2G/2G}^{\text{BS}}$ ), suppressing the ZLK effect and giving  $T_m/T_{\text{evap}} \gg 1$ . In contrast, the tidal capture channel dominates 2G/1G production due to the high 1G BH density, though most of these binaries also satisfy  $T_m/T_{\text{evap}} \gg 1$ , with only  $f_2 \lesssim 15\%$  entering the ZLK window where  $T_m \lesssim T_{\text{evap}}$ . For 1G/1G mergers, neither tidal capture nor binary–single channels are effective: tidal capture binaries are too compact ( $a_{1G/S}^{\text{tide}} \ll a_{2G/S}^{\text{tide}}$ ) and merge before further encounters, while systems formed in the binary–single channel experience weak ZLK excitation ( $a_{1G/1G}^{\text{BS}} \ll a_{2G/2G}^{\text{BS}}$ ). Only GW capture contributes significantly to 1G/1G mergers. As  $M_\bullet$  increases, the influence radius  $R_{\text{inf}}$  expands [94], shifting the active merger region outward and reducing merger rates. For  $M_\bullet \gtrsim 5 \times 10^7 M_\odot$ , only the GW capture channel remains viable. This is because the high velocity dispersion prolongs the encounter times, allowing binaries to merge before further interactions, while the larger galactic distances suppress the ZLK effect.

*Hierarchical mergers.*— In the hierarchical merger scenario, 1G BHs normally form with low spins ( $\chi \lesssim 0.3$ ) from stellar collapse [95]. A 1G/1G merger produces a 2G BH; for comparable mass progenitors, the merger remnant has a spin  $\simeq 0.7$  and the recoil velocity typically below 300km/s, allowing its retention in NSCs. However, mergers involving at least one high spin BH (e.g., 2G/1G or 2G/2G) yield 3G BHs with larger recoils.

Fig. 4 shows the distribution of merger kick versus final spin. As noted earlier, 2G/2G mergers in Milky Way-like galaxies primarily occur in the regions beyond 0.1 pc from the SMBH, where the local escape velocity  $v_s \lesssim 300$  km/s. For equal mass, equal spin binaries ( $\chi_{1,2} = 0.7$ ), about 75% of mergers have kicks above 300 km/s, and over 58% exceed 500 km/s. Most 3G BH remnants are therefore ejected from their host clusters, and their return through mass segregation is difficult, strongly suppressing further hierarchical growth.

*Conclusion and discussion.*— We have systematically investigated dynamical channels for 2G/2G mergers in nuclear star clusters, considering four distinct populations with fixed masses for simplicity: 2G BHs (massive BHs in the high-mass gap), 1G BHs (low-mass BHs), single stars, and binary stars. Our analysis reveals that 2G/2G mergers predominantly form through sequential binary–single interactions—beginning with 2G–binary star scattering, followed by 2G/star–star and 2G/star–2G encounters—that form wide 2G/2G binaries. These are subsequently driven to rapid merger by the SMBH-induced ZLK mechanism. The resulting merger rate depends sensitively on the assumed 2G BH

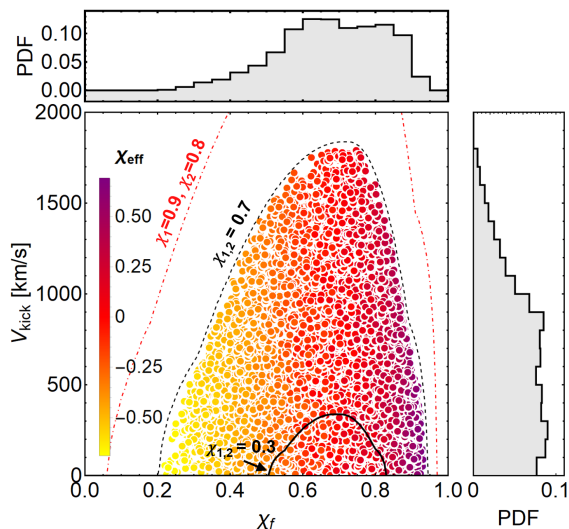


FIG. 4. Distribution of merger kick velocity versus final spin magnitude for equal-mass spinning BH mergers, assuming isotropic spin orientations (see the analytical fits in [96]). Color indicates the value of effective spin parameter  $\chi_{\text{eff}}$ , defined as  $\chi_{\text{eff}} = (m_1\chi_1\theta_1 + m_2\chi_2\theta_2)/(m_1 + m_2)$ , where  $\theta_{1,2}$  are the spin-orbit misalignment angles. The black dashed contour shows the boundary of distribution for the case of  $\chi_{1,2} = 0.7$ . For reference, the black solid contour corresponds to low spin case ( $\chi_{1,2} = 0.3$ ), and the red dot-dashed contours represent high unequal spins ( $\chi_1 = 0.9, \chi_2 = 0.8$ ).

number density  $f_{2G}$ , and generally is in agreement with that inferred for GW231123. This channel favors Milky Way-like galactic nuclei over more massive galaxies.

Nuclear star clusters are also efficient in producing 2G/1G binary mergers. Their relatively weak GW signals or large distances may hinder detection, but their long inspirals could make them promising low-frequency sources for future space-based detectors like LISA, Tianqin, and Taiji [97–99]. We further predict a significant population of 2G/star binaries, whose mergers could appear as micro tidal disruption events. Detecting these systems would help clarify 2G/2G formation pathways.

Our results indicate that 2G BHs likely originate from direct collapse of main-sequence stars into massive 1G BHs followed by binary evolution, not repeated low-mass 1G mergers. This is partly because low-mass 1G BHs merge inefficiently through typical dynamical processes, and partly because hierarchical mergers produce high-spin BHs with large kicks, ejecting them and suppressing further growth.

This theoretical framework, while adopting a number of simplified assumptions, can be extended to systems with continuous mass spectra. It may also provide physical insight into the origin of recent GW events such as GW241011 and GW241110 [100].

*Acknowledgments.*— B. L. thanks Wenbin Lu and Johan Samsing for useful discussions. B. L. acknowledges support from the National Key Research and Develop-

ment Program of China (No. 2023YFB3002502) and National Natural Science Foundation of China (Grant No. 12433008).

\* [liubin23@zju.edu.cn](mailto:liubin23@zju.edu.cn)

- [1] The LIGO Scientific Collaboration, the Virgo Collaboration, and the KAGRA Collaboration (LIGO Scientific, VIRGO, KAGRA), arXiv:2508.18083 (2025).
- [2] LIGO Scientific Collaboration and Virgo Collaboration, Phys. Rev. Lett. **125**, 101102 (2020).
- [3] The LIGO Scientific Collaboration, the Virgo Collaboration, and the KAGRA Collaboration (LIGO Scientific, VIRGO, KAGRA), arXiv:2507.08219 (2025).
- [4] V. M. Lipunov, K. A. Postnov, and M. E. Prokhorov, Astron. Lett. **23**, 492 (1997).
- [5] V. M. Lipunov, V. Kornilov, E. Gorbovskoy, D. A. H. Buckley, N. Tiurina, P. Balanutsa, A. Kuznetsov, J. Greiner, V. Vladimirov, D. Vlasenko et al., Mon. Not. R. Astron. Soc. **465**, 3656 (2017).
- [6] P. Podsiadlowski, S. Rappaport, and Z. Han, Mon. Not. R. Astron. Soc. **341**, 385 (2003).
- [7] K. Belczynski, M. Dominik, T. Bulik, R. O’Shaughnessy, C. Fryer, and D. E. Holz, Astrophys. J. Lett. **715**, L138 (2010).
- [8] K. Belczynski, D. E. Holz, T. Bulik, and R. O’Shaughnessy, Nature (London) **534**, 512 (2016).
- [9] M. Dominik, K. Belczynski, C. Fryer, D. E. Holz, E. Berti, T. Bulik, I. Mandel, and R. O’Shaughnessy, Astrophys. J. **759**, 52 (2012).
- [10] M. Dominik, K. Belczynski, C. Fryer, D. E. Holz, E. Berti, T. Bulik, I. Mandel, and R. O’Shaughnessy, Astrophys. J. **779**, 72 (2013).
- [11] M. Dominik, E. Berti, R. O’Shaughnessy, I. Mandel, K. Belczynski, C. Fryer, D. E. Holz, T. Bulik, and F. Pannarale, Astrophys. J. **806**, 263 (2015).
- [12] S. Stevenson, A. Vigna-Gómez, I. Mandel, J. W. Barrett, C. J. Neijssel, D. Perkins, and S. E. de Mink, Nature Commun. **8**, 14906 (2017).
- [13] B. Liu and D. Lai, Mon. Not. R. Astron. Soc. **502**, 2049 (2021).
- [14] J. Samsing and K. Hotokezaka, Astrophys. J. **923**, 126 (2021).
- [15] D. Gerosa and M. Fishbach, Nature Astron. **5**, 749 (2021).
- [16] Stegmann J., Olejak A., de Mink S. E., Astrophys. J. Lett. **992**, L26 (2025).
- [17] Kiroğlu F., Kremer K., Rasio F. A., arXiv:2509.05415 (2025).
- [18] Paiella L., Ugolini C., Spera M., Branchesi M., Arca Sedda M., arXiv:2509.10609 (2025).
- [19] Delfavero V., Ray S., Cook H. E., Nathaniel K., McKernan B., Ford K. E. S., Postiglione J., et al., arXiv:2508.13412 (2025).
- [20] Bartos I., Haiman Z., arXiv:2508.08558 (2025).
- [21] Passenger L., Banagiri S., Thrane E., Lasky P. D., Borchers A., Fishbach M., Ye C. S., arXiv:2510.14363 (2025).
- [22] Gottlieb O., Metzger B. D., Issa D., Li S. E., Renzo M., Isi M., arXiv:2508.15887 (2025).
- [23] C. Baruteau, J. Cuadra, and D. N. C. Lin, Astrophys.

- J. **726**, 28 (2011).
- [24] B. McKernan, K. E. S. Ford, W. Lyra, and H. B. Perets, *Mon. Not. Roy. Astron. Soc.* **425**, 460 (2012).
- [25] B. McKernan, K. E. S. Ford, J. Bellovary, N. W. C. Leigh, Z. Haiman, B. Kocsis, W. Lyra, M. M. MacLow, B. Metzger, M. O'Dowd, S. Endlich, and D. J. Rosen, *Astrophys. J.* **866**, 66 (2018).
- [26] I. Bartos, B. Kocsis, Z. Haiman, and S. Márka, *Astrophys. J.* **835**, 165 (2017).
- [27] N. C. Stone, B. D. Metzger, and Z. Haiman, *Mon. Not. Roy. Astron. Soc.* **464**, 946 (2017).
- [28] N. W. C. Leigh, A. M. Geller, B. McKernan, K. E. S. Ford, M. M. Mac Low, J. Bellovary, Z. Haiman, W. Lyra, J. Samsing, M. O'Dowd, B. Kocsis, and S. Endlich, *Mon. Not. Roy. Astron. Soc.* **474**, 5672 (2018).
- [29] B. Liu, D. Lai, and Y.-H. Wang, *Astrophys. J. Lett.* **883**, L7 (2019).
- [30] A. Secunda, J. Bellovary, M.-M. Mac Low, K. E. S. Ford, B. McKernan, N. W. C. Leigh, W. Lyra, and Z. Sándor, *Astrophys. J.* **878**, 85 (2019).
- [31] Y. Yang, I. Bartos, V. Gayathri, K. E. S. Ford, Z. Haiman, S. Klimentenko, B. Kocsis, S. Márka, Z. Márka, B. McKernan, and R. O'Shaughnessy, *Phys. Rev. Lett.* **123**, 181101 (2019).
- [32] B. Liu, and D. Lai, *Phys. Rev. D* **102**, 023020 (2020).
- [33] M. Gröbner, W. Ishibashi, S. Tiwari, M. Haney, and P. Jetzer, *Astron. Astrophys.* **638**, A119 (2020).
- [34] W. Ishibashi and M. Gröbner, *Astron. Astrophys.* **639**, A108 (2020).
- [35] H. Tagawa, Z. Haiman, and B. Kocsis, *Astrophys. J.* **898**, 25 (2020).
- [36] H. Tagawa, B. Kocsis, Z. Haiman, I. Bartos, K. Omukai, J. Samsing, *Astrophys. J.* **908**, 194 (2021).
- [37] H. Tagawa, B. Kocsis, Z. Haiman, I. Bartos, K. Omukai, J. Samsing, *Astrophys. J. Lett.* **907**, L20 (2021).
- [38] H. Tagawa, Z. Haiman, I. Bartos, B. Kocsis, K. Omukai, *Mon. Not. Roy. Astron. Soc.* **507**, 3362 (2021).
- [39] Y. P. Li, A. M. Dempsey, S. Li, H. Li, and J. Li, *Astrophys. J.* **911**, 124 (2021).
- [40] K. E. S. Ford and B. McKernan, arXiv:2109.03212 [astro-ph.HE] (2021).
- [41] J. Samsing, I. Bartos, D. J. D'Orazio, Z. Haiman, B. Kocsis, N. W. C. Leigh, B. Liu, M. E. Pessah, and H. Tagawa, *Nature*, **603**, 237 (2022).
- [42] R. Li and D. Lai, arXiv:2202.07633 [astro-ph.HE] (2022).
- [43] J. Li and D. Lai, arXiv:2203.05584 [astro-ph.HE] (2022).
- [44] D. Chattopadhyay, J. Stegmann, F. Antonini, J. Barber, I. M. Romero-Shaw, *Mon. Not. Roy. Astron. Soc.* **526**, 4908 (2023).
- [45] Y. Su, C. Rowan, M. Rozner, *Mon. Not. R. Astron. Soc.* **543**, 1864 (2025).
- [46] M. Rozner, E. Ramirez-Ruiz, *Astrophys. J. Lett.* **988**, L21 (2025).
- [47] S. F. P. Zwart and S. L. W. McMillan, *Astrophys. J. Lett.* **528**, L17 (2000).
- [48] R. M. O'Leary, F. A. Rasio, J. M. Fregeau, N. Ivanova, and R. O'Shaughnessy, *Astrophys. J.* **637**, 937 (2006).
- [49] M. C. Miller and V. Lauburg, *Astrophys. J.* **692**, 917 (2009).
- [50] S. Banerjee, H. Baumgardt, and P. Kroupa, *Mon. Not. R. Astron. Soc.* **402**, 371 (2010).
- [51] J. M. B. Downing, M. J. Benacquista, M. Giersz, and R. Spurzem, *Mon. Not. R. Astron. Soc.* **407**, 1946 (2010).
- [52] B. M. Ziosi, M. Mapelli, M. Branchesi, and G. Tormen, *Mon. Not. R. Astron. Soc.* **441**, 3703 (2014).
- [53] C. L. Rodriguez, M. Morscher, B. Pattabiraman, S. Chatterjee, C.-J. Haster, and F. A. Rasio, *Phys. Rev. Lett.* **115**, 051101 (2015).
- [54] J. Samsing and E. Ramirez-Ruiz, *Astrophys. J. Lett.* **840**, L14 (2017).
- [55] J. Samsing and D. J. D'Orazio, *Mon. Not. R. Astron. Soc.* **481**, 5445 (2018).
- [56] C. L. Rodriguez, P. Amaro-Seoane, S. Chatterjee, and F. A. Rasio, *Phys. Rev. Lett.* **120**, 151101 (2018).
- [57] L. Gondán, B. Kocsis, P. Raffai, and Z. Frei, *Astrophys. J.* **860**, 5 (2018).
- [58] M. Rozner, H. B. Perets, *Astrophys. J.* **931**, 149 (2022).
- [59] H. von Zeipel, *Astronomische Nachrichten* **183**, 345 (1910).
- [60] M. L. Lidov, *Planetary and Space Science* **9**, 719 (1962).
- [61] Y. Kozai, *Astron. J.* **67**, 591 (1962).
- [62] S. Naoz, *Annu. Rev. Astron. Astrophys.* **54**, 441 (2016).
- [63] M. C. Miller and D. P. Hamilton, *Astrophys. J.* **576**, 894 (2002).
- [64] L. Wen, *Astrophys. J.* **598**, 419 (2003).
- [65] F. Antonini and H. B. Perets, *Astrophys. J.* **757**, 27 (2012).
- [66] F. Antonini, S. Toonen, and A. S. Hamers, *Astrophys. J.* **841**, 77 (2017).
- [67] K. Silsbee and S. Tremaine, *Astrophys. J.* **836**, 39 (2017).
- [68] C. Petrovich and F. Antonini, *Astrophys. J.* **846**, 146 (2017).
- [69] B. Liu and D. Lai, *Astrophys. J.* **863**, 68 (2018).
- [70] L. Randall and Z.-Z. Xianyu, *Astrophys. J.* **853**, 93 (2018).
- [71] B.-M. Hoang, S. Naoz, B. Kocsis, F. A. Rasio, and F. Dosopoulou, *Astrophys. J.* **856**, 140 (2018).
- [72] B. Liu and D. Lai, *Mon. Not. R. Astron. Soc.* **483**, 4060 (2019).
- [73] G. Fragione and B. Kocsis, *Mon. Not. R. Astron. Soc.* **486**, 4781 (2019).
- [74] G. Fragione, E. Grishin, N. W. C. Leigh, H. B. Perets, and R. Perna, *Mon. Not. R. Astron. Soc.* **488**, 47 (2019).
- [75] M. Zevin, J. Samsing, C. Rodriguez, C.-J. Haster, and E. Ramirez-Ruiz, *Astrophys. J.* **871**, 91 (2019).
- [76] T. Alexander, *ARA&A* **55**, 17 (2017).
- [77] J. N. Bahcall and R. A. Wolf, *Astrophys. J.* **209**, 214 (1976).
- [78] R. Genzel, F. Eisenhauer, and S. Gillessen, *Rev. Mod. Phys.* **82**, 3121 (2010).
- [79] T. Alexander, *Astrophys. J.* **527**, 835 (1999).
- [80] T. Alexander and O. Pfuhl, *Astrophys. J.* **780**, 148 (2014).
- [81] I. Linial, R. Sari, *Astrophys. J.* **940**, 101 (2022).
- [82] B. Rom, I. Linial, R. Sari, *Astrophys. J.* **951**, 14 (2023).
- [83] B. Rom and R. Sari, *Astrophys. J.* **991**, 146 (2025).
- [84] P. C. Peters, *Phys. Rev.* **136**, B1224 (1964).
- [85] S. F. Portegies Zwart and A. T. Meinen, *Astron. Astrophys.* **280**, 174 (1993).
- [86] D. Lai, *Astrophys. J.* **490**, 847 (1997).
- [87] J. Binney and S. Tremaine, *Galactic dynamics* (1987).
- [88]  $T_{\text{evap}}$  adopted in our model refers to  $T_{\text{evap}} \simeq (m_{2G}/m_s)^2 T_{2G/2G-S}$ , in which  $T_{2G/2G-S}$  denotes the timescale for a 2G/2G binary to interact with a field star, i.e.,  $T_{2G/2G-S} = [n_s \pi (4G m_{2G} a_{2G/2G} / v_s +$

$a_{2G/2G}^2 v_s]^{-1}$ . If the second term in the bracket is neglected, our expression for  $T_{\text{evap}}$  reduces to the same order-of-magnitude estimate as that used in [87].

- [89] F. Yu, D. Lai, *Astrophys. J.* **977**, 268 (2024).  
 [90] B. Liu, D. J. Muñoz, and D. Lai, *Mon. Not. Roy. Astron. Soc.* **447**, 747 (2015).  
 [91] To account for the ZLK effect, we model the 2G/2G binary as moving on a moderately eccentric orbit (eccentricity  $\sim 0.5$ ) around the central SMBH.  
 [92] M. R. Blanton et al. (SDSS), *Astrophys. J.* **592**, 819 (2003).  
 [93] Joop Schaye et al., *Mon. Not. R. Astron. Soc.* **446**, 521 (2014).  
 [94] S. Tremaine, K. Gebhardt, R. Bender, G. Bower, A. Dressler, S. M. Faber, A. V. Filippenko, R. Green, C. Grillmair, L. C. Ho, J. Kormendy, T. R. Lauer, J. Magorrian, J. Pinkney, and D. Richstone, *Astrophys. J.* **574**, 740 (2002).  
 [95] J. Fuller and L. Ma, *Astrophys. J. Lett.* **881**, L1 (2019).  
 [96] C. O. Lousto, M. Campanelli, Y. Zlochower, and H. Nakano, *Class. Quant. Grav.* **27**, 114006 (2010).  
 [97] P. Amaro-Seoane, H. Audley, S. Babak, J. Baker, E. Barausse, P. Bender, E. Berti, P. Binétruy et al., arXiv:1702.00786 [astro-ph.IM] (2017).  
 [98] J. Luo, L.-S. Chen, H.-Z. Duan, Y.-G. Gong, S. Hu, J. Ji, Q. Liu, J. Mei, V. Milyukov, M. Sazhin, C.-G. Shao, V. T. Toth, H.-B. Tu, Y. Wang, Y. Wang, H.-C. Yeh, M.-S. Zhan, Y. Zhang, V. Zharov, and Z.-B. Zhou, *Classical and Quantum Gravity* **33**, 035010 (2016).  
 [99] W.-R. Hu and Y.-L. Wu, *National Science Review* **4**, 685 (2017).  
 [100] The LIGO Scientific Collaboration, the Virgo Collaboration, and the KAGRA Collaboration (LIGO Scientific, VIRGO, KAGRA), *Astrophys. J. Lett.* **993**, L21 (2025).

### A: Merger rate

This section presents the merger rate calculations used in the main text for a typical galaxy. For the GW capture channel, 2G BHs evolve through three stages into 3G BHs (see Fig. 1 in the main text). We track three “intermediate populations” as: (1) single 2G BHs,  $N_{2G}$ ; (2) 2G/2G binary,  $N_{2G/2G}$ ; and (3) 3G BHs,  $N_{3G}$ . Their evolution is described by:

$$\begin{cases} \frac{dN_{2G}}{dt} = -\frac{N_{2G}}{T_{2G-2G}} + \left(\frac{dN_{2G}}{dt}\right)_{\text{source}} \simeq 0 \\ \frac{dN_{2G/2G}}{dt} = \frac{N_{2G}}{T_{2G-2G}} - \frac{N_{2G/2G}}{T_m} \\ \frac{dN_{3G}}{dt} = \frac{N_{2G/2G}}{T_m}, \end{cases}$$

where the initial value  $N_{2G}(0) = N_{2G0} \neq 0$ ,  $N_{2G/2G}(0) = N_{3G}(0) = 0$ . The solution is:

$$\begin{cases} N_{2G}(t) = N_{2G0} \\ N_{2G/2G}(t) = \frac{N_{2G0} T_m}{T_{2G-2G}} \left(1 - e^{-t/T_m}\right). \end{cases}$$

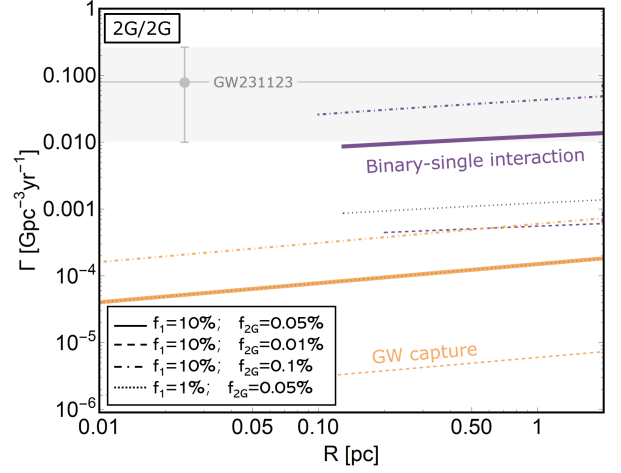


FIG. 5. Merger rate of 2G/2G binaries versus galactocentric distance  $R$ . Since Eqs. (15) and (16) give the merger rate per galaxy, we rescale the rate to  $\text{Gpc}^{-3}\text{yr}^{-1}$  using the number density of Milky Way-like galaxies for comparison with the GW231123 detection rate ( $0.08_{-0.07}^{+0.19}\text{Gpc}^{-3}\text{yr}^{-1}$ ) [3, 92, 93]. Different values of  $f_1$  and  $f_{2G}$  are considered as labeled. For the GW capture channel,  $T_m$  in Eq. (15) is the merger time of an isolated binary [84]. For the binary–single channel, ZLK oscillations induced by the SMBH can accelerate 2G/2G mergers.  $T_m$  in Eq. (16) is set to  $T_{\text{evap}}$ , and  $f_2$  denotes the numerically evaluated fraction of systems with  $T_m \lesssim T_{\text{evap}}$  [13].

The resulting merger rate of 2G/2G BHB at distance  $R$  is given by:

$$\Gamma = \frac{dN_{3G}}{dt} = \frac{dN_{2G0}}{d \ln R} \frac{1}{T_{2G-2G}} \left(1 - e^{-\frac{T_H}{T_m}}\right). \quad (15)$$

Here, we set  $t = T_H = 10^{10}$  yrs.

For the tidal capture and binary–single interaction channels, as mentioned in the main text, an additional stage of 2G/S binary formation is included, leading to the following extended set of equations:

$$\begin{cases} \frac{dN_{2G}}{dt} = -\frac{N_{2G}}{T_A} + \left(\frac{dN_{2G}}{dt}\right)_{\text{source}} \simeq 0 \\ \frac{dN_{2G/S}}{dt} = \frac{N_{2G}}{T_A} - \frac{N_{2G/S}}{T_B} \\ \frac{dN_{2G/2G}}{dt} = f_1 \frac{N_{2G/S}}{T_B} - \frac{N_{2G/2G}}{T_m} \\ \frac{dN_{3G}}{dt} = f_2 \frac{N_{2G/2G}}{T_m}. \end{cases}$$

where  $T_A \equiv T_{2G-S}$  (tidal capture) or  $T_{2G-S/S}$  (binary single interaction), and  $T_B \equiv T_{2G/S-2G}$ . Since  $N_{2G}$  is a constant, we can find the analytical solution as follows:

$$\begin{cases} N_{2G}(t) = N_{2G0} \\ N_{2G/S}(t) = \frac{N_{2G0} T_B}{T_A} \left(1 - e^{-\frac{t}{T_B}}\right) \\ N_{2G/2G}(t) = f_1 \frac{N_{2G0} T_m}{T_A} \left(1 + \frac{T_m e^{-\frac{t}{T_m}} - T_B e^{-\frac{t}{T_B}}}{T_B - T_m}\right) \end{cases}$$

Then, for a given distance  $R$ , the merger rate is

$$\Gamma = \frac{dN_{2G0}}{dl n R} \frac{f_1 f_2}{T_A} \left( 1 + \frac{T_m e^{-\frac{T_H}{T_m}} - T_B e^{-\frac{T_H}{T_B}}}{T_B - T_m} \right). \quad (16)$$

The parameter  $f_1$  in Eq. (16) represents the probability that a 2G/S binary forms a 2G/2G binary after interacting with another 2G BH. Its value depends on the three-body mass and orbital properties during the encounter, and should ideally be determined via N-body simulations. The parameter  $f_{2G} = n_s/n_{2G}$  denotes the abundance ratio of 2G BHs to stars, which can vary the encounter timescale. For the fiducial example in the main text, we adopt fixed values of  $f_1 = 10\%$  and  $f_{2G} = 0.05\%$ .

As shown in Fig. 5, we examine the dependence of  $\Gamma$  on these parameters. We see that the merger rate  $\Gamma$  depends linearly on  $f_1$  for the binary-single channel, while it is highly sensitive to  $f_{2G}$ . To compare with the observed rate of GW231123, we rescale  $\Gamma$  by considering the number of Milky Way-like galaxy within a  $\lesssim 4\text{Gpc}^3$  volume (i.e.,  $\sim 10^7$ ) [92, 93]. We find that such channel is able to predict a merger rate in agreement with the detection rate of GW231123 when the 2G BH fraction  $f_{2G} \gtrsim 0.05\%$ .

## B: Mergers from 2G/1G binaries

*Channel 1: Gravitational wave capture.* This channel follows a similar dynamical process as the 2G/2G case. Consider a gravitationally focused encounter between a 2G BH and a 1G BH, with pericenter distance  $r_{\text{int}}^{\text{GW}}$ . The timescale for such encounters is given by

$$T_{2G-1G} \simeq v_s [2\pi G(m_{2G} + m_{1G})n_{1G}r_{\text{int}}^{\text{GW}}]^{-1}. \quad (17)$$

During the close passage, energy is radiated via GWs. The amount of energy dissipated is approximately  $\Delta E_{\text{GW}} \simeq (85\pi/12\sqrt{2})[G^{7/2}\mu_{2G,1G}^2(m_{2G} + m_{1G})^{5/2}]/[c^5(r_{\text{int}}^{\text{GW}})^{7/2}]$ . A bound 2G/1G binary forms if the total energy after the encounter becomes negative, i.e.,  $(1/2)\mu_{2G,1G}v_{2G}^2 - \Delta E_{\text{GW}}(r_{\text{int}}) = E_b \equiv -Gm_{2G}m_{1G}/(2a_{2G/1G}) \lesssim 0$ . Moreover, for the binary to survive subsequent stellar interactions without being disrupted, its binding energy must satisfy  $E_b \lesssim -m_s v_s^2/2$ . This defines the characteristic semi-major axis:

$$a_{2G/1G}^{\text{GW}} \simeq \frac{Gm_{2G}m_{1G}}{m_s v_s^2}. \quad (18)$$

The interaction radius  $r_{\text{int}}^{\text{GW}}$  is determined by setting the GW energy loss comparable to the binding energy requirement ( $\Delta E_{\text{GW}} \simeq m_s v_s^2$ ):

$$r_{\text{int}}^{\text{GW}} \equiv \left( \frac{85\pi}{12\sqrt{2}} \right)^{2/7} \left[ \frac{c^2 m_{1G}^2 (m_{1G} + m_{2G})^{1/2}}{v_s^2 m_s m_{2G}^{3/2}} \right]^{2/7} R_g, \quad (19)$$

where  $R_g = Gm_{2G}/c^2$  is the gravitational radius of the 2G BH. The characteristic eccentricity of the newly formed binary can be determined using the relation  $a_{2G/1G}^{\text{GW}}(1 - e_{2G/1G}^{\text{GW}}) \simeq r_{\text{int}}^{\text{GW}}$ .

*Channel 2: Tidal capture.* A 2G BH can also form a binary with a 1G BH through an intermediate tidal capture step. In this two-step process, a 2G BH first tidally captures a star to form a 2G/S binary. The timescale for such a 2G-S encounter follows the same formulation as in the 2G/2G case. The characteristic semi-major axis of the resulting 2G/S binary is

$$a_{2G/S}^{\text{tide}} \simeq \frac{Gm_{2G}}{v_s^2}. \quad (20)$$

Subsequent gravitational scatterings with passing stars harden this binary, reducing its semi-major axis to  $a_{2G/S}^{\prime\text{tide}} \simeq a_{2G/S}^{\text{tide}}/2$ . A 2G/1G binary may then form via a binary-single exchange interaction when a 1G BH approaches the hardened 2G/star binary within a distance  $\sim a_{2G/S}^{\prime\text{tide}}$ . The timescale for this encounter is

$$T_{2G/S-1G} \simeq v_s [2\pi G(m_{2G} + m_{1G})n_{1G}a_{2G/S}^{\prime\text{tide}}]^{-1}. \quad (21)$$

During this interaction, an energy exchange of order  $\Delta E \simeq Gm_{2G}m_s/a_{2G/S}^{\prime\text{tide}}$  occurs. If the total energy becomes negative, a 2G/1G binary forms, ejecting the lighter star. The binding energy of the newly formed binary satisfies  $G(m_{2G} + m_{1G})/(2a_{2G/1G}) \simeq \Delta E/2$ , giving a characteristic semi-major axis:

$$a_{2G/1G}^{\text{tide}} \simeq \frac{Gm_{1G}}{v_s^2} \frac{m_{2G}}{m_s}. \quad (22)$$

The corresponding eccentricity follows from  $a_{2G/2G}^{\text{tide}}(1 - e_{2G/2G}^{\text{tide}}) \simeq a_{2G/S}^{\prime\text{tide}}$ . The resulting 2G/1G binary is relatively soft and could be disrupted by subsequent scatterings. We therefore only consider binaries that merge within the evaporation timescale  $T_{\text{evap}}$ .

*Channel 3: Binary-single interaction.* A third channel for 2G/1G mergers arises from binary-single interactions, particularly between a 2G BH and a stellar binary. This process is analogous to the 2G/2G case, except that the encounter between a 2G/S binary and another 2G BH is replaced with interactions between a 2G/S binary and a 1G BH. The characteristic semi-major axis of the 2G/star binary formed through this channel is

$$a_{2G/S}^{\text{BS}} \simeq \frac{Gm_s}{v_s^2} \left( \frac{m_{2G}}{m_s} \right)^{2/3}. \quad (23)$$

After hardening via scattering with field stars to  $a_{2G/S}^{\prime\text{BS}} \simeq a_{2G/S}^{\text{BS}}/2$ , the binary may encounter a 1G BH. During this interaction, an energy exchange of order  $\Delta E \simeq Gm_{2G}m_s/a_{2G/S}^{\prime\text{BS}}$  occurs, potentially forming a 2G/1G binary. If  $G(m_{2G} + m_{1G})/(2a_{2G/1G}) \simeq \Delta E/2$ , the characteristic semi-major axis of the resulting 2G/1G binary is:

$$a_{2G/1G} \simeq \frac{Gm_{1G}}{v_s^2} \left( \frac{m_{2G}}{m_s} \right)^{2/3}. \quad (24)$$

As with the other channels, the resulting 2G/1G binary is subject to disruptive encounters, and only those merging within  $T_{\text{evap}}$  contribute to the merger rate calculations.